Extended Poisson's ratio range in chiral isotropic elastic materials

R. S. Lakes* B. Huey and K. Goyal

Department of Engineering Physics and Department of Materials Science,
University of Wisconsin, Madison, WI 53706
* rlakes@wisc.edu

September 12, 2023

Abstract

Poisson's ratio in chiral Cosserat elastic solids is considered. Chirality allows the Poisson's ratio to exceed classical bounds, even if the material is directionally isotropic and all elastic moduli are within thermodynamic limits based on strain energy density. Poisson's ratio in chiral rods depends on the chiral elastic constants as well as on the shear and bulk moduli, assumed positive. Poisson's ratio can be greater than 0.5 or smaller than -1 for slender chiral specimens.

1 Introduction and rationale

Classically isotropic elastic solids have two independent elastic constants. At least four constants are used: the Young's modulus, shear modulus, bulk modulus and Poisson's ratio. They are interrelated so only two are independent. The range of Poisson's ratio inferred from energy relations associated with stability is from -1 to 0.5 for isotropic materials in three dimensions [1]. By now, negative Poisson's ratio materials [2] are well known [3, 4, 5]. Chirality, which admits a distinction between left and right handed microstructure, has no effect in classical elasticity because the elastic modulus tensor is fourth rank.

The Cosserat [6] theory of elasticity provides more freedom than classical elasticity. The range of Poisson's ratio for an isotropic Cosserat solid is the same as that for a classical solid. Non-chiral Cosserat solids are predicted to exhibit size effects [7]. Many experiments on non-chiral heterogeneous materials have been done, enabling the Cosserat elastic constants to be extracted (see [8] and references therein).

Chiral structure on the scale of atomic structure in molecules has long been known to have effects in chemistry [9]. In crystals and crystalline materials, chirality is associated with physical properties such as piezoelectricity, pyroelectricity, and optical activity [10]. Chiral materials are also called noncentrosymmetric or hemitropic. Classical elasticity provides no distinction between left and right handed materials but Cosserat elasticity [6] also (with a micro-inertia term) called micropolar elasticity [11], has sufficient freedom to accommodate chirality. Chiral Cosserat solids can support initial stresses and skin effects [12]. Analysis of chiral Cosserat elasticity [13] has enabled interpretation of experiments that disclose coupling between extension or compression and twist deformation. Experiments reveal that designed chiral rib [14] [15] [16] lattices and surface [17]

lattices exhibit coupling between axial compression and twist as anticipated by analysis of a chiral Cosserat elastic rod. Bone [18] tendon [19] and liquid crystal elastomers [20] also exhibit stretch-twist coupling. Size effects in Poisson's ratio of chiral lattices have been observed; the magnitude of these size effects depends on the lattice. Analysis of two dimensional negative Poisson's ratio chiral lattices revealed a Cosserat characteristic length comparable to the cell size [21]. Chiral nano-wires [22] exhibited size dependent effects and surface effects. Chiral Cosserat solids have also been predicted to exhibit coupling between temperature changes and twist deformation [23]. The objective of this study is to explore the influence of the chiral Cosserat elastic constants on size effects in Poisson's ratio.

2 Analysis

2.1 Chiral elastic solids

Chirality is incorporated in linear Cosserat elasticity via the following constitutive equations [13]. The material is assumed to be isotropic with respect to direction. Chiral solids are not invariant to inversions of coordinates.

$$\sigma_{kl} = \lambda\epsilon_{rr}\delta_{kl} + 2G\epsilon_{kl} + \kappa e_{klm}(r_m - \phi_m) + \\ C_1\phi_{r,r}\delta_{kl} + C_2\phi_{k,l} + C_3\phi_{l,k} \tag{1}$$

$$m_{kl} = \alpha\phi_{r,r}\delta_{kl} + \beta\phi_{k,l} + \gamma\phi_{l,k} + C_1\epsilon_{rr}\delta_{kl} + \\ (C_2 + C_3)\epsilon_{kl} + (C_3 - C_2)e_{klm}(r_m - \phi_m) \tag{2}$$

The stress σ_{ij} (force per unit area) in a Cosserat solid can be asymmetric. Moments per unit area m_{kl} balance the asymmetry. ϵ_{kl} is the strain tensor. e_{klm} is the permutation symbol. The macro-rotation is $r_i = (e_{ijk}u_{k,j})/2$ with u as displacement; ϕ_k is the micro-rotation which is the rotation of points.

G is the shear modulus in the absence of gradients. Elastic constant λ has the same meaning as in classical elasticity. Elastic constants α, β, γ are Cosserat elastic constants that quantify sensitivity to gradients of local rotation. Elastic constant κ quantifies the coupling between local rotation and rotation due to displacement gradient. Elastic constants C_1, C_2 and C_3 quantify the effect of chirality.

Characteristic lengths are defined to provide physical insight. When a length scale in an experiment begins to approach a characteristic length, nonclassical effects including size effects in bending and torsion [7] and reduction in stress concentration factors [24] [25] are predicted. The characteristic length for torsion is $\ell_t = \sqrt{\frac{\beta+\gamma}{2G}}$, and for bending, $\ell_b = \sqrt{\frac{\gamma}{4G}}$.

The radial deformation of a chiral circular cylinder in response to an axial strain e is given [13] by

$$u_r(r) = -(\nu_0 r + A_9\frac{C_1 + C_2 + C_3}{e(\lambda + 2G)}I_1(pr))e \tag{3}$$

in which $p^2 = \frac{2\kappa}{\alpha+\beta+\gamma}\frac{1}{1-K_0^2}$ and $I_1(pr)$ is the modified Bessel function of first order; r is the radial coordinate and K_0 is defined below. There is assumed to be no constraint upon rotation of the ends. Nonclassical effects including stretch-twist coupling and size effects in Poisson's ratio depend on the chiral elastic constants C_1, C_2 and C_3. The Poisson effect contains a component of homogeneous deformation and a heterogeneous component of deformation that depends on radial coordinate

2

r. The solution also contains a circumferential component of displacement that corresponds to coupling between the applied stretch or squeeze deformation and a twisting response given by

$$u_\theta(r) = b_0 r z e \tag{4}$$

in which b_0 is a function of the elastic constants. Because the strain is incorporated here, the expression for b_0 in [13] must be modified by factoring out the strain.

The homogeneous contribution in Equation 3 to the Poisson's ratio of the chiral solid is given by

$$\nu_0 = \frac{\begin{vmatrix} (\ell_0^2 + (R/2)^2)(R^2/2) & -\ell_2 R^2/2 & \ell_3^2 A_{11} - K_1^2(\ell_2^2 + \ell_3^2)A_{11} + K_5 A_{12} \\ (K_2 - 1)/2 & -K_3 K_0/\ell_4 & A_{30}(1 - K_0^2) + (K_2 - K_1^2)I_1(pR)/R \\ (K_3 - 1)/2 & -K_4/K_0\ell_4 & (K_3 - K_4)I_1(pR)/R \end{vmatrix}}{\begin{vmatrix} (\ell_0^2 + (R/2)^2)(R^2/2) & -\ell_2 R^2 & \ell_3^2 A_{11} - K_1^2(\ell_2^2 + \ell_3^2)A_{11} + K_5 A_{12} \\ (K_2 - 1)/2 & -K_0(K_3 + 1)/\ell_4 & A_{30}(1 - K_0^2) + (K_2 - K_1^2)I_1(pR)/R \\ (K_3 - 1)/2 & -(K_4 + 1)/K_0\ell_4 & (K_3 - K_4)I_1(pR)/R \end{vmatrix}} \tag{5}$$

in which $A_{11} = R I_1(pR)$, $A_{12} = R^2 I_2(pR)/p$ and $A_{30} = (pI_0(pR)) - I_1(pR)/R)$ with I_0, I_1 and I_2 as the modified Bessel function of order 0, 1, and 2 respectively. The strain e has been factored from columns in the determinants in [13] and divided for simplicity. The material is linear so Poisson and other effects are independent of strain.

A_9 in Equation 3 describing the heterogeneous contribution to Poisson's ratio depends on the elastic constants and the radius as follows.

$$A_9 = \frac{e \begin{vmatrix} (\ell_0^2 + (R/2)^2)(R^2/2) & -\ell_2 R^2 & -\ell_1 R^2/2 \\ (K_2 - 1)/2 & -K_0(K_3 + 1)/\ell_4 & -K_3 K_0/\ell_4 \\ (K_3 - 1)/2 & -(K_4 + 1)/K_0\ell_4 & -K_4/K_0\ell_4 \end{vmatrix}}{\begin{vmatrix} (\ell_0^2 + (R/2)^2)(R^2/2) & -\ell_2 R^2 & \ell_3^2 A_{11} - K_1^2(\ell_2^2 + \ell_3^2)A_{11} + K_5 A_{12} \\ (K_2 - 1)/2 & -K_0(K_3 + 1)/\ell_4 & A_{30}(1 - K_0^2) + (K_2 - K_1^2)I_1(pR)/R \\ (K_3 - 1)/2 & -(K_4 + 1)/K_0\ell_4 & (K_3 - K_4)I_1(pR)/R \end{vmatrix}} \tag{6}$$

The predicted Poisson's ratio is determined at the surface, $r = R$, where measurements are done. In the determinant in the denominator, the subscript of K_2 in the third column, second row had been omitted in [13]. This typographical error is corrected here.

2.2 Physical meaning of constants

As for elastic constants in relation to constants in Equation 1 and in Equation 2, Young's modulus is $E = \frac{G(3\lambda + 2G)}{\lambda + G}$. The classical Poisson's ratio is $\nu = \frac{\lambda}{2\lambda + 2G}$.

The quantity $2\mu + \kappa$ in the earlier notation used by A. C. Eringen [11] and other writers [13] corresponds to $2G$ in which G is the classical shear modulus in the absence of gradients. This earlier notation, if used, requires caution [26].

The characteristic length for torsion $\ell_t = \sqrt{\frac{\beta + \gamma}{2G}}$ corresponds to ℓ_0 in the chiral analysis. This characteristic length quantifies the length scale at which Cosserat effects become prominent. If the experimental length scale is less than about a factor 20 greater than the characteristic length, Cosserat effects are observable.

The characteristic length $\ell_4^2 = \frac{\alpha + \beta + \gamma}{\lambda + 2G}$ in the chiral analysis may be written $\ell_4^2 = \frac{\ell_t^2}{\Psi} \frac{1 - 2\nu}{1 - \nu}$.

3

As for dimensionless coupling constants, K_0 is a dimensionless measure of the degree of chiral coupling; it is given by $K_0^2 = \frac{(C_1+C_2+C_3)^2}{(\alpha+\beta+\gamma)(\lambda+2G)}$. This may be expressed $K_0^2 = (C_1 + C_2 + C_3)^2 \Psi \frac{1}{\ell_t^2} \frac{1}{2G^2} \frac{1-2\nu}{1-\nu}$.

$K_1 = K_0\sqrt{K_3}$ is a related dimensionless measure of the degree of chiral coupling.

$K_2 = \frac{\alpha}{\alpha+\beta+\gamma}$ is a dimensionless ratio of isotropic Cosserat elastic constants that represent rotation sensitivity.

The polar ratio $\Psi = \frac{\beta+\gamma}{\alpha+\beta+\gamma}$ is a dimensionless ratio of rotation gradient sensitivity elements; it is analogous to Poisson's ratio in classical elasticity. Its allowable range is from 0 to 1.5. Because $K_2 = \frac{\alpha}{\alpha+\beta+\gamma}$, we have $K_2 = 1 - \Psi$.

$K_3 = \frac{C_1}{C_1+C_2+C_3}$ is a dimensionless ratio of chirality coefficients.

$K_4 = \frac{\lambda}{\lambda+2G}$. Because the classical Poisson's ratio is $\nu = \frac{\lambda}{2\lambda+2G}$, $K_4 = \frac{\nu}{1-\nu}$.

$K_5 = \frac{\kappa}{2G} = \frac{N^2}{1-N^2}$ in which the coupling number $N = \sqrt{\frac{\kappa}{2G+\kappa}}$ represents the degree of coupling between macro and micro rotations. Nonclassical effects such as size effects [7] and reduction is stress concentration factor [25] are known to increase with N.

2.3 Stability considerations

As for the classical constants, an unconstrained specimen of an isotropic classical solid will be stable provided the shear modulus G and the bulk modulus $B = \lambda + 2G/3$ are positive. This range corresponds to an assumption of a positive definite strain energy [1]. The corresponding range for Poisson's ratio ν is $-1 < \nu < \frac{1}{2}$.

For isotropic Cosserat solids, stability analysis via an assumption of positive definite strain energy [11] provides $\infty > \kappa > 0$; $\gamma > 0$; $-\gamma < \beta < \gamma$; $3\alpha + \beta + \gamma > 0$. These imply $\ell_b^2 > 0$, $\ell_t^2 > 0$ and $1 > N^2 > 0$; also $0 < \Psi < 3/2$.

For directionally isotropic chiral solids, similar stability analysis [13] provides

$$K_{10}^2 = \frac{(C_2 + C_3)^2}{4(2G)(\beta + \gamma)} < 1 \tag{7}$$

$$K_{11}^2 = \frac{(C_2 - C_3)^2}{4(2G)(\gamma - \beta)} < 1 \tag{8}$$

$$K_{12}^2 = \frac{(3C_1 + C_2 + C_3)^2}{4(3\lambda + 2G)(3\alpha + \beta + \gamma)} < 1. \tag{9}$$

In the present study, all elastic constants have been assumed to be within the above stability limits. For finite size objects of a Cosserat solid, less stringent conditions may apply [27] [28]. The reason is that that terms containing elastic constants are assumed to be independent and uncoupled in the stability analyses but in Cosserat solid objects of finite size, the variables are in fact coupled. Materials near the limits of stability with $N = 1$ are predicted to exhibit folding and faulting phenomena [29, 30].

3 Results: Poisson effect

The following plots show Poisson's ratio vs. specimen radius for several ranges of parameters. It is initially assumed that $\alpha = 0$, so $\Psi = 1$. It is also assumed that $\ell_t = 5$ mm and that $\beta/\gamma = 0.99$. We assume also $\kappa = 33G$ for the present study of Poisson's ratio. Large κ has been assumed

for analysis of experiments on stretch twist coupling [14]. Observe that $\kappa \to \infty$ implies $p \to \infty$ in which κ quantifies the coupling between micro and macro rotations. This also corresponds to $N \to 1$, consistent with observation for some of the lattices we have studied. The case $N \to 1$ also maximizes Cosserat size effects and reductions in stress concentration factor.

Variation in C_1 is considered first with $C_2 = C_3 = 0$. Different classical Poisson's ratios are assumed. Observe in Figure 1 that if the classical Poisson's ratio is from 0.35 to 0.45 the effect of chirality via variation of C_1 is minimal. As the classical Poisson's ratio becomes smaller, the effect of chirality is larger. If the classical Poisson's ratio is negative, there is a pronounced effect of chirality for sufficiently small specimens as shown in Figure 1.
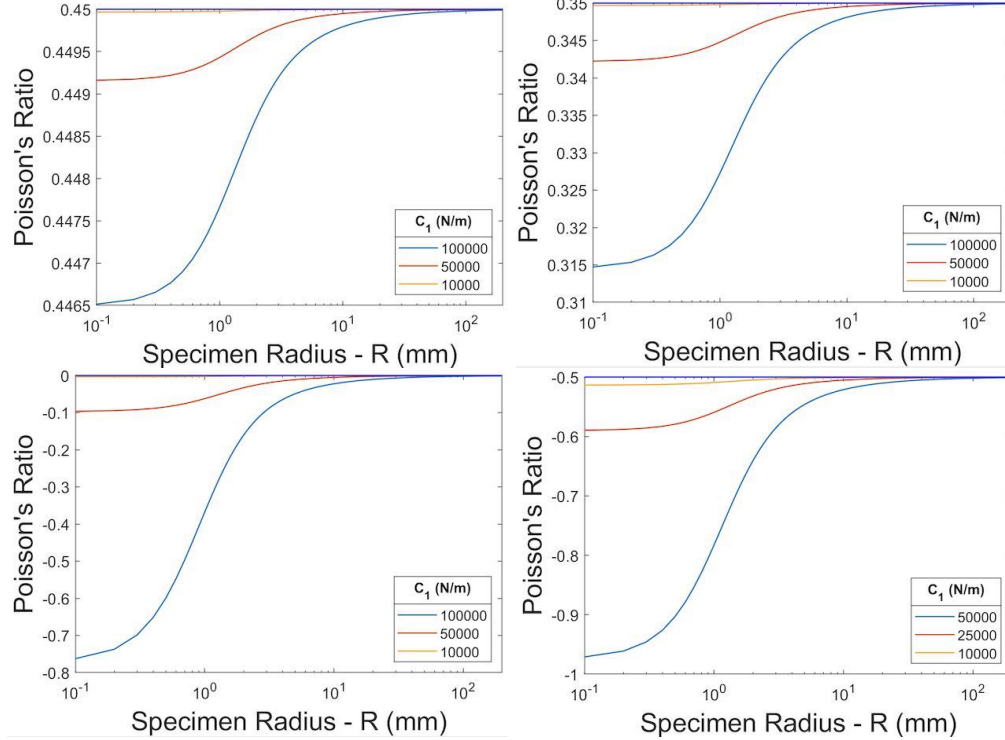
Figure 1: Poisson's ratio vs. radius for various C_1; classical Poisson's ratio 0.45, 0.35, 0, -0.5. Poisson's ratio is independent of size in classical solids and non-chiral Cosserat solids as indicated by the horizontal line.

Poisson's ratio can be below -1, the classical lower limit, as shown in Figure 2. If C_1 is increased to 75000 N/m, Poisson's ratio decreases to -36 but only for the smallest radius in the range. If $C_1 < 0$, the Poisson's ratio excursion is not as negative as it is for positive C_1. An increase in α also reduces the variation in Poisson's ratio with radius.

Variation of C_2 with $C_1 = C_3 = 0$ has considerably less effect on Poisson's ratio than variation of C_1 as shown in Figure 3.

If $\beta = 0$, then one can allow larger values of C_2 and remain within the stability limits (see Equation 8). For a starting classical Poisson's ratio of 0.45, and with $C_3 = -0.9C_2$ and with $C_1 = 0$, the chirality allows the Poisson's ratio to exceed 0.5 as shown in Figure 4. If $C_2 < 0$ with the above assumptions, Poisson's ratio tends to negative values for small R.

The characteristic length ℓ_t larger be considerably than the microstructure size, permitting experiments on specimens with $R > \ell_t$ as demonstrated by experiments on foams.
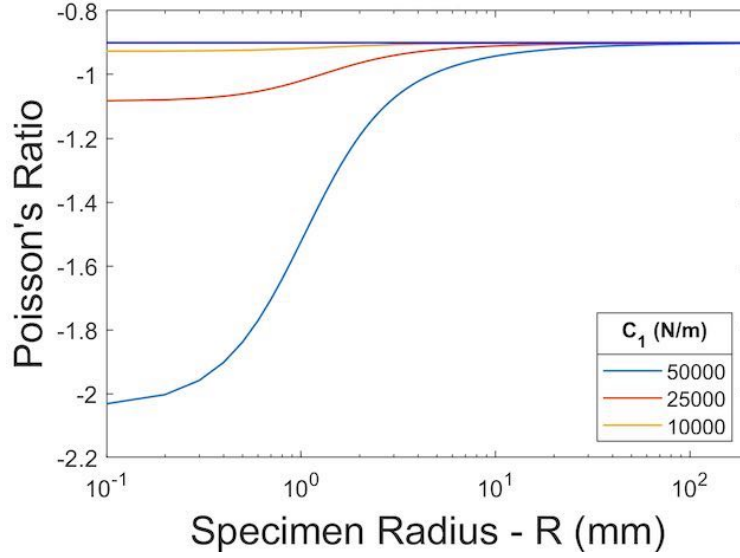
Figure 2: Poisson's ratio vs. radius for various C_1; classical Poisson's ratio -0.9. Poisson's ratio is independent of size in classical solids and non-chiral Cosserat solids as indicated by the horizontal line.
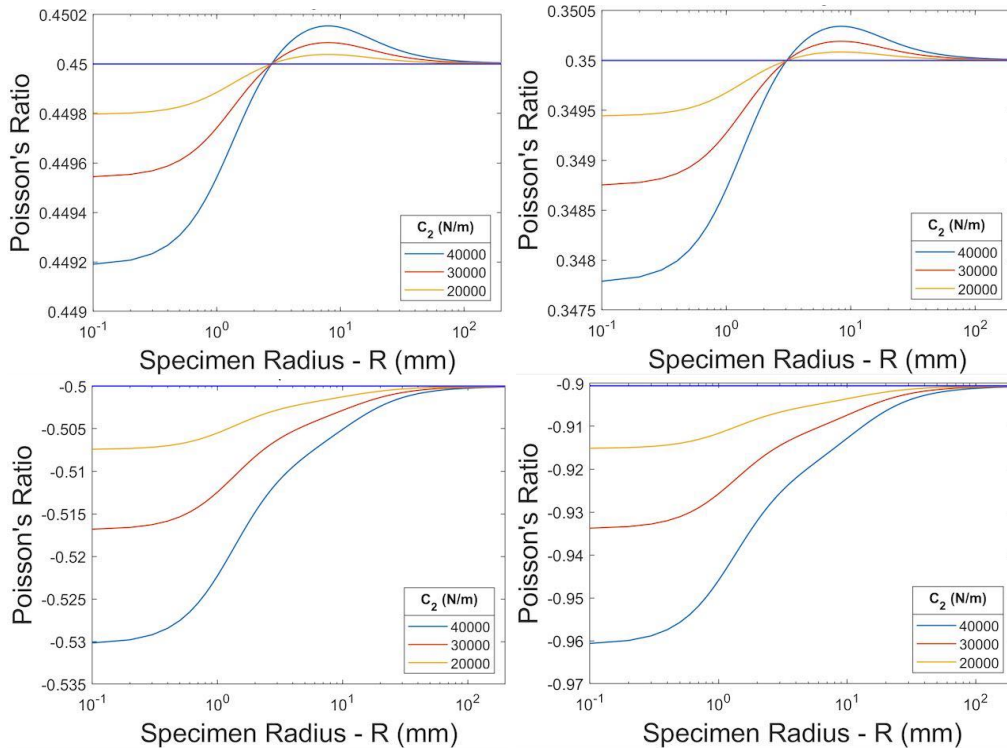
Figure 3: Poisson's ratio vs. radius for various C_2; classical Poisson's ratio 0.45, 0.35, -0.5, –0.9. Poisson's ratio is independent of size in classical solids and non-chiral Cosserat solids as indicated by the horizontal line.
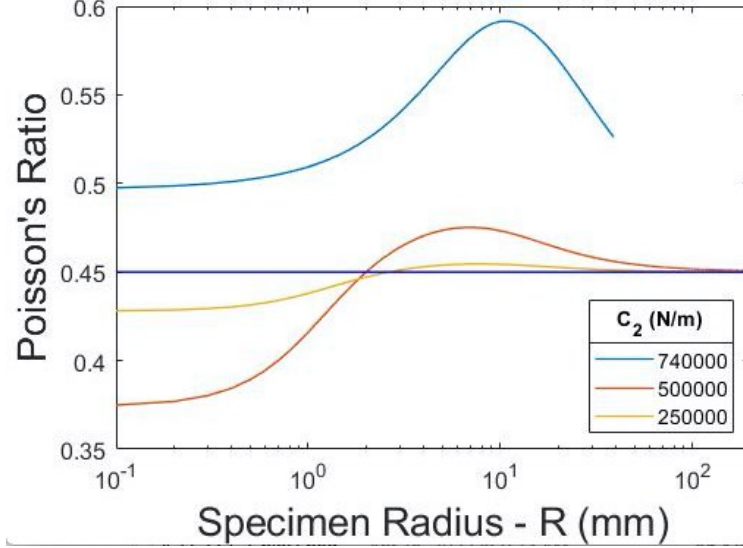
Figure 4: Poisson's ratio vs. radius for various C_2 with $C_3 = -0.9C_2$; classical Poisson's ratio 0.45. Poisson's ratio is independent of size in classical solids and non-chiral Cosserat solids as indicated by the horizontal line.

4   Discussion and Conclusions

The classical range of Poisson's ratio is derived from the assumption of positive definite strain energy which requires the bulk and shear moduli to be positive. It is also tacitly assumed that bulk and shear deformations are independent. In a chiral solid, there is stretch-twist coupling so these deformations are linked and are not independent. The Poisson's ratio predicted in a chiral solid differs from the assumed classical value which is always taken to be within the classical stability range. No internal energy has been added to obtain Poisson's ratios outside the classical range. All assumed moduli are within classic stability ranges. This is in contrast to the approach taken in composites with a negative stiffness constituent [31].

Expansion of the Poisson's ratio range is considered to arise from oblique redirection of forces applied during compression or tension. Observe that C_1 couples the dilatational part of the deformation field to the couple stress in Equation 2. When the classical Poisson's ratio is negative, the material is compliant in dilatation compared to shear, so chirality via C_1 has a substantial influence. By contrast, C_2 and C_3 couple the shear part of the deformation; the effect on Poisson's ratio is smaller than that of C_1 as shown in Figure 3. If one allows larger values of C_2 via choosing $\beta = 0$ and if one maximizes $C_3 - C_2$, then Poisson's ratio can exceed 0.5 as shown in Figure 4. In this example the classical Poisson's ratio is large so the material is compliant in shear compared with dilatation.

As for comparison with experiment, chiral cubic lattices designed for negative Poisson's ratio exhibited squeeze twist coupling [14]. Poisson's ratio in these lattices was negative and exhibited a pronounced size dependence. Chiral gyroid lattices were observed to exhibit squeeze-twist coupling [15]. Poisson's ratio of the gyroid lattice was about 0.3 with little dependence on radius in contrast to the above.

It is concluded that chirality allows Poisson's ratio of directionally isotropic solids to exceed classical bounds, even if all elastic moduli are within thermodynamic limits based on strain energy

density. Poisson's ratio can be greater than 0.5 or smaller than -1 if the chiral specimen is sufficiently slender.

5   Acknowledgment

References

[1] I. S. Sokolnikoff, *Theory of Elasticity*, Krieger; Malabar, FL, (1983).

[2] R. S. Lakes, Foam structures with a negative Poisson's ratio, Science, 235, 1038-1040, (1987).

[3] R. S. Lakes, Negative-Poisson's-ratio materials: auxetic solids, Annual Review of Materials Research, 47, 63-81 (2017).

[4] K. W. Wojciechowski, Poisson's ratio of anisotropic systems, Computational Methods in Science and Technology (CMST) 11 (1), 73-79 (2005)

[5] C. Branka, D. M. Heyes, K. W. Wojciechowski, Auxeticity of cubic materials, Physica Status Solidi, 246, 9, 2063-2071 (2009).

[6] E. Cosserat and F. Cosserat, *Theorie des Corps Deformables*, Hermann et Fils, Paris (1909).

[7] R. D. Gauthier and W. E. Jahsman, A quest for micropolar elastic constants. J. Applied Mechanics, 42, 369-374 (1975).

[8] Z. Rueger and R. S. Lakes, Strong Cosserat elasticity in a transversely isotropic polymer lattice, Physical Review Letters, 120, 065501 Feb. (2018).

[9] R. Bentley, From optical activity in quartz to chiral drugs: molecular handedness in biology and medicine, Perspect. Biol. Med. 38 (2), 188-229 (1995).

[10] J. F. Nye, *Physical Properties of Crystals*, Oxford, Clarendon, (1976).

[11] A. C. Eringen, Theory of micropolar elasticity. In *Fracture* Vol. 1, 621-729 (edited by H. Liebowitz), Academic Press, New York (1968).

[12] Y. Weitsman, Initial stresses and skin effects in a hemitropic Cosserat continuum, J. Appl. Mech. Trans. ASME, 34, 160-164 (1967).

[13] R. S. Lakes, and R. L. Benedict, Noncentrosymmetry in micropolar elasticity. Int. J. Engng. Sci. 20, 1161-1167 (1982).

[14] C. S. Ha, M. E. Plesha, R. S. Lakes, Chiral three-dimensional isotropic lattices with negative Poisson's ratio, Physica Status Solidi B, 253, (7), 1243-1251 (2016).

[15] D. Reasa and R. S. Lakes, Cosserat effects in achiral and chiral cubic lattices, Journal of Applied Mechanics (JAM), 86, 111009, 6 pages Nov. (2019).

[16] C. S. Ha, R. S. Lakes, M. E. Plesha, Observation of squeeze twist coupling in a chiral three-dimensional isotropic lattice, Physica Status Solidi B 257, (10), 1900140, (2020)

[17] D. R. Reasa and R. S. Lakes, Nonclassical chiral elasticity of the gyroid lattice, Phys. Rev. Lett. 125, 205502 (2020).

[18] R. S. Lakes, Is bone elastically noncentrosymmetric?, Proc. 34th ACEMB. Houston (1981).

[19] K. Buchanan, R. S. Lakes, R. Vanderby, Chiral behavior in rat tail tendon fascicles, Journal of Biomechanics, 64, 206-211 (2017).

[20] M. Warner, E. M. Terentjev, R. B. Meyer, and Y. Mao, Untwisting of a cholesteric elastomer by a mechanical field, Phys. Rev. Lett. 102, 217601 (2009).

[21] A. Spadoni and M. Ruzzene, Elasto-static micropolar behavior of a chiral auxetic lattice, J. Mechanics and Physics of Solids, 60, 156-171 (2012).

[22] J. S. Wang, T. Shimada, G. F. Wang and T. Kitamura, Effects of chirality and surface stresses on the bending and buckling of chiral nanowires, J. Phys. D: Appl. Phys. 47 015302 (5pp) (2014)

[23] D. Iesan, Thermal effects in chiral elastic rods, International Journal of Thermal Sciences, 49, 1593-1599, (2010).

[24] R. D. Mindlin, Influence of couple stresses on stress concentrations, Exp. Mech. 3, 1-7 (1963).

[25] T. Ariman, On the stresses around a circular hole in micropolar elasticity, Acta. Mech. IV, 216-229 (1967).

[26] S. C. Cowin, An incorrect inequality in micropolar elasticity theory, Zeitschrift für angewandte Mathematik und Physik (ZAMP) 21, 494-497 (1970).

[27] O. Brulin and S. Hjalmars, Stability conditions in continuum models of discrete systems, in *Continuum Models of Discrete Systems 4*, eds. O. Brulin and R. K. T. Hsieh, p. 209-212, North Holland Publishing, Amsterdam, (1981).

[28] R. S. Lakes, Stability of Cosserat solids: size effects, ellipticity and waves, Journal of mechanics of materials and structures (JoMMS), 13 (1) 83-91 (2018).

[29] P. A. Gourgiotis and D. Bigoni, Stress channelling in extreme couple-stress materials Part I: Strong ellipticity, wave propagation, ellipticity, and discontinuity relations. Journal of the Mechanics and Physics of Solids 88, 150-168 (2016).

[30] P. A. Gourgiotis and D. Bigoni, The dynamics of folding instability in a constrained Cosserat medium, Philosophical Transactions of the Royal Society A, A 375: 20160159 (2017).

[31] T. Jaglinski, D. S. Stone, D, Kochmann, and R. S. Lakes, Materials with viscoelastic stiffness greater than diamond, Science, 315, 620-622, (2007).